Journal of Biostatistics and Epidemiology

J Biostat Epidemiol. 2024;10(4): 448-460

Original Article

Machine Learning Models for Prognostic Assessment of Covid-19 Mortality Using Computed Tomography-Based Radiomics

Nima Yousefi, Vahid Ghavami, Maryam Salari, Saeed Akhlaghi*

Department of Biostatistics, School of Health, Mashhad University of Medical Sciences, Mashhad, Iran.

ARTICLE INFO

Received 19.06.2024
Revised 13.07.2024
Accepted 15.08.2024
Published 15.12.2024

Key words:
Machine learning;
Radiomics features;
Computed tomography scan;
Mortality;
Covid-19

ABSTRACT

Introduction: This study examines the significance of developing a predictive approach for assessing the prognosis of individuals diagnosed with COVID-19. This method can help physicians make treatment decisions that decrease mortality and prevent unnecessary treatments. This study also emphasizes the significance of radiomics features. Therefore, our objective was to assess the predictive capabilities of Computed Tomography-based radiomics models using a dataset comprising 577 individuals diagnosed with COVID-19.
Methods: The U-net model was applied to automatically perform whole lung segmentations, extracting 107 texture, intensity, and morphological features. We utilized two feature selectors and three classifiers. We assessed the random forest, logistic regression, and support vector machines by implementing a five-fold cross-validation approach. Precision, sensitivity, specificity, accuracy, F1-score, and area under the receiver operating characteristic curve were reported.
Results: The random forest model achieved an area under the receiver operating characteristic curve, precision, sensitivity, specificity, accuracy, and F1-score in the range of 0.85 (CI 95%: 0.76–0.91), 0.75, 0.82, 0.78, 0.68, and 0.71, respectively. Logistic regression attained an area under the receiver operating characteristic curve of 0.80 (CI 95%: 0.72–0.88), corresponding to values of 0.88, 0.62, 0.74, 0.55, and 0.67, respectively. Support Vector Machines computed the above six metrics as an area under the receiver operating characteristic curve, sensitivity, specificity, accuracy, precision, and F1-score in the range of 0.69 (CI 95%: 0.59–0.79), 0.68, 0.64, 0.66, 0.5, and 0.57, respectively.
Conclusion: We are developing a robust radiomics classifier that predicts mortality in COVID-19 patients. Lung Computed Tomography radiomics features may aid in identifying high-risk individuals who need supplementary therapy and decrease the propagation of the virus.

Introduction

The coronavirus family comprises viruses mostly responsible for inducing human respiratory illnesses, including pneumonia, bronchitis, and acute chronic respiratory distress syndrome. During the first stage, infected persons have a substantial surge in viral production in their upper respiratory tract, which promotes the transmission of the virus

*.Corresponding Author: Akhlaghis@mums.ac.ir

to others.[1] By July 23, 2020, the World Health Organization acknowledged that COVID-19 had disseminated to more than 170 countries, affecting over 15 million individuals globally and formally leading to 619,000 recorded deaths.[2] On January 22, 2023, the global tally of afflicted individuals was 664 million, resulting in nearly 6.7 million deaths. Also, mortality reported in the Eastern Mediterranean region, which includes Iran, exceeded 349 thousand due to this disease.[3] Medical experts have suggested utilizing image processing methods to predict COVID-19 mortality.[4] Technological advancements and the growth of data science have inundated the world with vast amounts of data across multiple scientific disciplines. The analysis and interpretation of large datasets necessitate novel and intricate methodologies to extract valuable information to predict disease mortality most straightforwardly.[5] Some patients may need access to medical records, which can prevent using methods that rely on demographic and clinical factors to predict mortality. Additionally, errors may arise during the gathering and assessment of these variables.[6] Machine learning algorithms utilizing image processing techniques can achieve this goal. The images were preserved in their Digital Imaging and Communications in Medicine (DICOM) format to ensure quality. The necessary features for analyzing and predicting mortality were extracted from these images.

Materials and methods

This research is a cross-sectional study that investigates patients who were hospitalized with COVID-19 at Imam Reza and Qaem hospitals in Mashhad, Razavi Khorasan Province, from 2020 to January 2022. The flowchart of the current study protocol is shown in Figure 1. This research received clearance from the School of Public Health ethics committee at Mashhad University of Medical Sciences in Iran (approval no IR.MUMS.FHMPM.

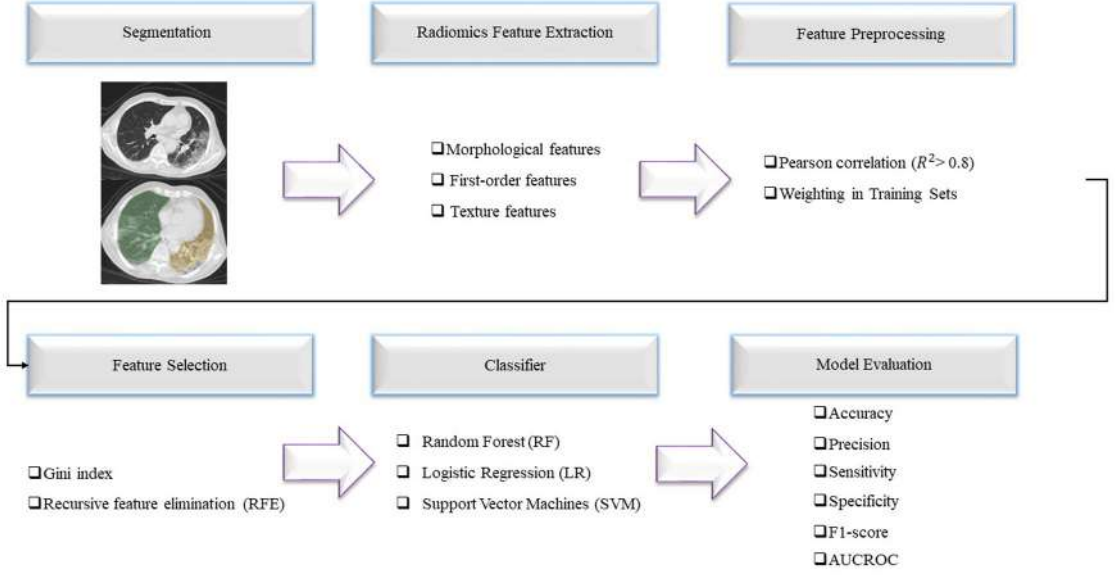

Figure 1. Flowchart of the current study protocol

REC.1401.221). It adhered to the stipulations of the Helsinki Declaration. Informed consent was obtained from all participants for participation in the study.

Study population

This study was conducted on all individuals suspected or confirmed to have COVID-19. A physician's diagnosis relied on a positive Reverse Transcription Polymerase Chain Reaction (RT-PCR) test and a Computed Tomography scan (CT-scan). These individuals were explicitly admitted to the hospital for this purpose. Between March 2020 and January 2022, systematic sampling was used to identify 1100 patients from a pool of 6271 hospitalized patients with confirmed COVID-19. Thirty-two participants were removed from the study due to the absence of a high-resolution computed tomography scan (HRCT) and were substituted with other individuals. Out of a total of 1068 DICOM images, 119 were removed due to their unclear nature and inability to be processed. The study comprised 577 patients who possessed comprehensive data out of the remaining 949 samples. Among the patients, 380 have recovered, while 197 have been deceased. In addition, CT images were promptly obtained upon patients' arrival at the hospital. Figure 2 displays examples of the images within the dataset for both Recovered and Deceased COVID-19 patients.

Image segmentation and image preprocessing

U-Net, an automated technique based on deep learning, segmented the lungs.[7] It has a U-shaped structure with a contracting path and an expansive path also known as an encoder and a decoder respectively. Through convolutional layers and max pooling operations, the encoder gradually decreases spatial dimensions while increasing feature depth to capture contextual information. The decoder uses transposed convolutions to up-sample these feature maps back to the original image size and add skip connections from the encoder to preserve detailed spatial information. The capacity of U-Net to function well with little annotated data and its efficiency in maintaining fine details through skip connections are two of

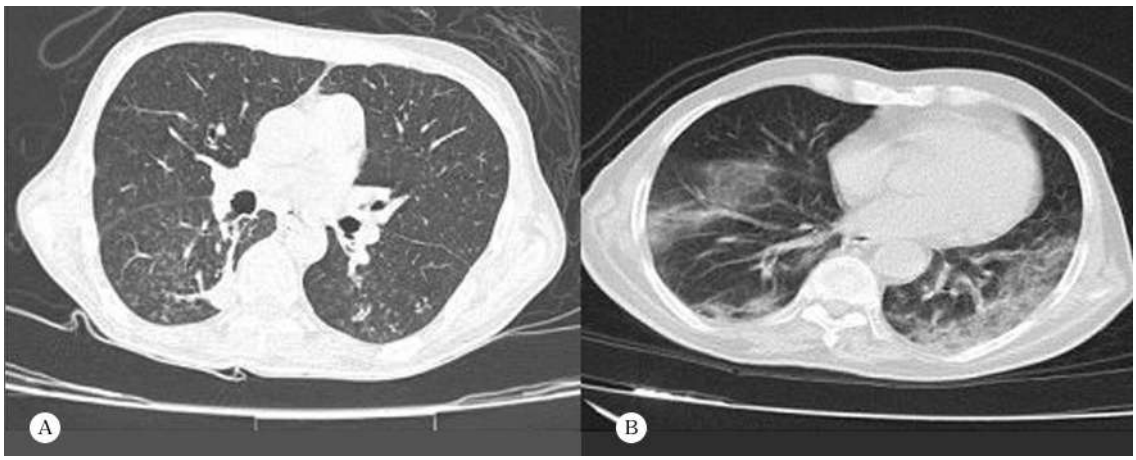

Figure 2. Samples of the CT images dataset. (a) images of recovered COVID-19 patients, (b) images of deceased COVID-19 patients.

its main characteristics. Furthermore, the CT images maintained their original proportions. The entire image was normalized by centering it at the mean with standard deviation. After the segmentation check, the image voxel size was changed to have equal dimensions in all directions, specifically 1 × 1 × 1. Additionally, the image's intensity was divided into 42 equal bins.[8]

Feature Extraction Techniques

Using quantitative characteristics derived from radiological images is advancing quickly in artificial intelligence.[9] The investigation began by extracting attributes from images. The Pyradiomics library[10] is an essential Python software tool for extracting radiomics features from medical images. radiomics features were extracted according to the guidelines set by the Image Biomarker Standardization Initiative (IBSI).[11] These features include shape, statistical, and texture features.[12] The texture features encompass various matrices, including the Grey Level Size Zone Matrix (GLSZM), Grey Level Co-occurrence Matrix (GLCM), Neighboring Gray Tone Difference Matrix (NGTDM), Grey Level Run Length Matrix (GLRLM), and Grey Level Dependence Matrix (GLDM).[13] All 107 features, along with their names and definitions, are available in the Supplementary Data.

Feature preprocessing

The correlation between the features was assessed by applying the Pearson correlation. Features exhibiting a high correlation (> 0.8) were eliminated. Due to an imbalanced dataset in both the training and test sets, the weighting approach was applied only to the training set for each model.[14]

Machine learning algorithms

Following the extraction of features, the subsequent stage involved training machine learning models and assessing their performance using test sets. This study utilized the most powerful and widely used machine learning algorithms. The machine learning algorithms employed for classification were logistic regression (LR), random forest (RF), and support vector machines (SVM).

Logistic Regression

LR is one of the statistical approaches used in machine learning. In this model, the outcome is a binary variable, and the independent variable can be any of the quantitative, ordinal, or nominal. This model predicts a probability that belongs to a particular category with a number between 0 and 1.[15]

Random Forest

RF includes combination algorithms that use decision trees as simple and weaker learners. As a result, a group of trees decides to form a forest, and its decision-making abilities surpass those of an individual tree. Each of the algorithms performs a learning operation after receiving the data. Every one of these algorithms predicts a specific outcome.[16] The RF algorithm can ultimately choose, by voting, the group that has won the most votes and place it as the final class. Moreover, this model is superior to other machine learning models due to its straightforward implementation and

decreased hyperparameter constraints.[17]

Support Vector machines

SVM is an architecture that classifies data into two groups by assessing the distance of individual data points from each category, identifying the central point between the two groups, and determining the best hyperplane.[18] The hyperplane is . The weights vector is denoted as , the features vector as x, and the bias as b.[19]

Model evaluation

RF, LR, and SVM models were constructed to determine an approach for classifying patients in the training dataset. Radiomics features were also computed for each individual image. The predictive performance was evaluated in terms of area under curve (AUC), sensitivity, specificity, accuracy, precision, and F1 score. The larger the AUC, the higher the prediction accuracy.

Result

Table 1 presents a concise overview of the characteristics of the population, including age, gender, intensive care unit (ICU), length of stay, and comorbidities. The clinical attribution of patient mortality to COVID-19 disease was established. Among the 577 patients studied, 311 were male, and 266 were female. The mean age of recovered patients was 57.57, while that of deceased patients was 67.17. Age is significantly associated with mortality (P<0.001). Of male patients, 199 recovered, and

Table 1. Demographic and Clinical characteristics of COVID-19 patients

Patient Characteristics	Outcome		P-value
	(197=N) Deceased	(380=N) Recovered	
Age	16.09±67.17	17.03± 57.57	<0.001[a]
Sex (Male)	(56.09) 112	199 (52.4)	<0.306[a]
Smoking	1 (0.5)	8 (2.1)	0.142[b]
Hospital Length of Stay	7 (11)	6 (5)	0.077[a]
Admitted to ICU	123 (62.4)	49 (12.9)	<0.001[a]
Abdominal pain	0 (0.0)	7 (1.8)	0.102[b]
Vomiting	8 (4.1)	24 (6.3)	0.282[a]
Diarrhea	3 (1.6)	6 (1.6)	>0.999[b]
Anorexia	17 (8.8)	58 (15.3)	0.030[a]
Cancer	8 (4.1)	1 (0.3)	0.001[b]
Liver Disease	0 (0.0)	1 (0.3)	>0.999[b]
Diabetes	27 (13.7)	60 (15.8)	0.507[a]
Cardiovascular Disease	10 (5.1)	30 (7.9)	0.206[a]
Asthma	3 (1.5)	4 (1.1)	0.695[b]
Blood pressure	38 (19.3)	79 (20.8)	0.671[a]

[a], Mann-Whitney U test; [b], Fisher exact test
Description as mean standard deviation for quantitative variables that follow a normal distribution, median (Interquartile range) for non-normal distributed quantitative variables, and count (percentage) for qualitative variables.

112 deceased. There is no significant association between sex and mortality (P=0.306); among those with diabetes, 60 recovered, and 27 deceased. There is no significant difference between diabetes and mortality (P=0.507).

Results were gathered by Python 3.8, scikit-learn 1.0.3, seg-metrics 1.2.8, and Pyradiomics 3.0.1. U-Net output was validated with dice similarity coefficient (DSC) and average symmetry surface distance (ASSD). The DSC and ASSD values were obtained as follows: Dice, 0.97±0.06 (mean±SD); ASSD, 0.862±0.2 mm.

RF, LR, and SVM were used for classification. For model fitting, hyperparameters were tuned. Grid search and 5-fold stratified cross-validation were used. The specified hyperparameters were presented in Table 2.

The assessment of the model is a crucial component of any study. We employed the 5-fold cross-validation technique in our study to obtain more accurate and dependable results. The evaluation procedure for the model performance utilized metrics such as AUC, Precision, Specificity, Sensitivity, accuracy, and F1 score.

The confusion matrix was computed for all the classifiers to illustrate the percentage variations in True Positives (TP), True Negatives (TN), False Positives (FP), and False Negatives (FN). The results were reported in Table 3. Among the 107 features group, after removing highly correlated features, as depicted in Figure 3, 33 different features remained based on their importance coefficient. The training phase of our predictive model utilized features as inputs, with death being the only outcome. The distribution of the top 10 most important features is illustrated in Figure 4.

The prognostic performance of each machine learning algorithm was evaluated for patient outcome prediction. Table 4 and Figure 5 show the evaluated performance of each machine learning model constructed using radiomics features. As a result of performance verification, the RF model AUC, accuracy, sensitivity, specificity, precision, and F1-score were 0.85 (CI 95%: 0.76–0.91), 0.78, 0.75, 0.82, 0.68, and 0.71, respectively. The LR model AUC, accuracy, sensitivity, specificity,

Table 2. The hyperparameters of Random Forest, Logistic Regression, and Support Vector Machines models.

Model	Hyperparameters
RF	Min samples split: 10, Min samples leaf: 3, Number of estimators: 100, class weight: balanced
LR	C: 1, penalty: L2, max iteration: 1000, class weight: balanced
SVM	Number of features to select: 24, C: 1000, class weight: balanced

Table 3. Confusion Matrix of Random Forest, Logistic Regression, and Support Vector Machines on the test set. The values of the confusion matrix are expressed as Counts and percentages

	Model		
	RF	LR	SVM
True positive (%)	30 (26)	35 (30)	27 (23)
False positive (%)	14 (12)	29 (25)	27 (23)
True negative (%)	62 (53)	47 (41)	49 (43)
False negative (%)	10 (9)	5 (4)	13 (11)

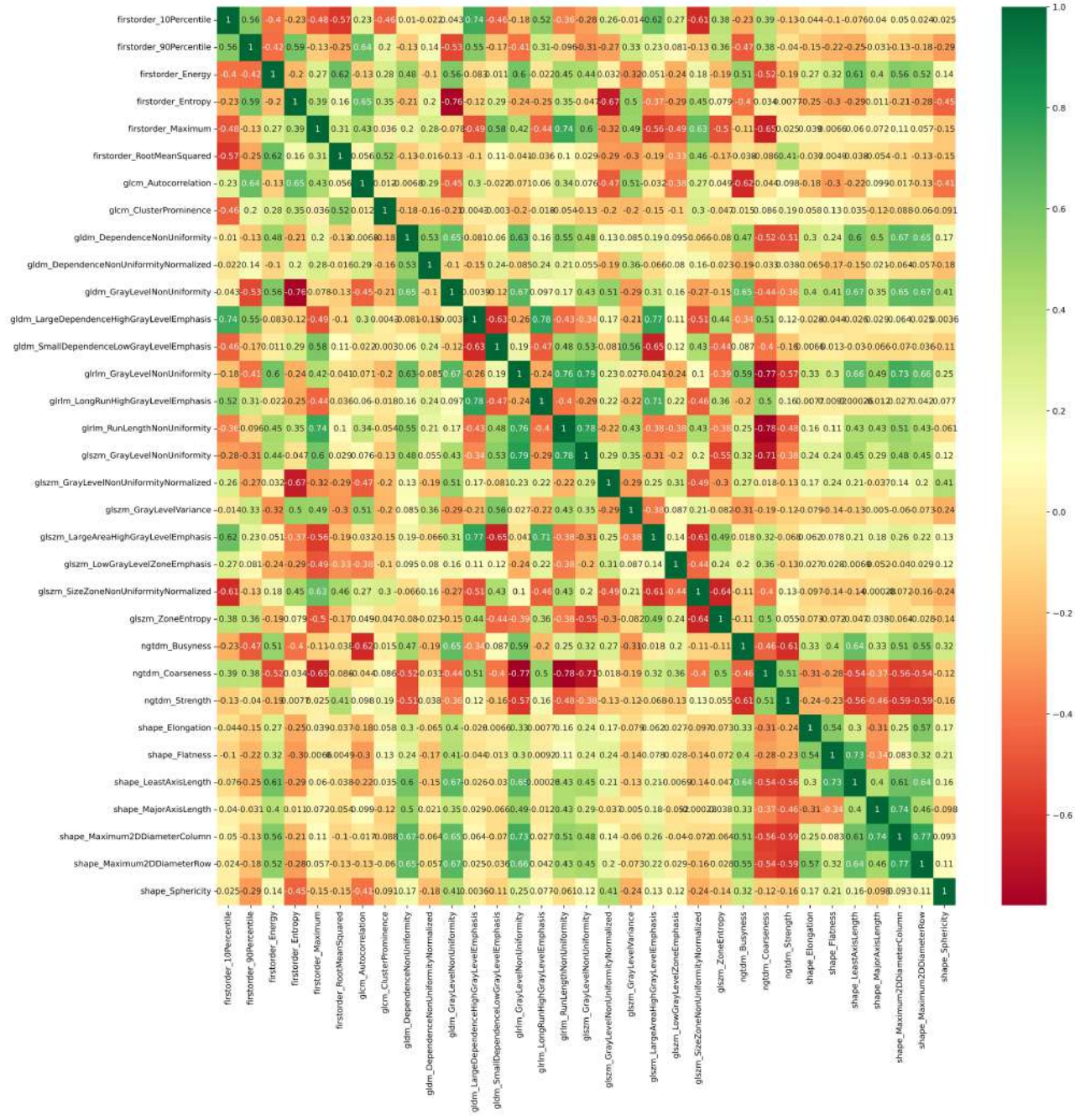

Figure 3. Heatmap showing the effect of the features on the training of each machine learning model. The higher the heatmap value, the stronger the influence of the feature on the differentiation between the recovered and diseased groups.

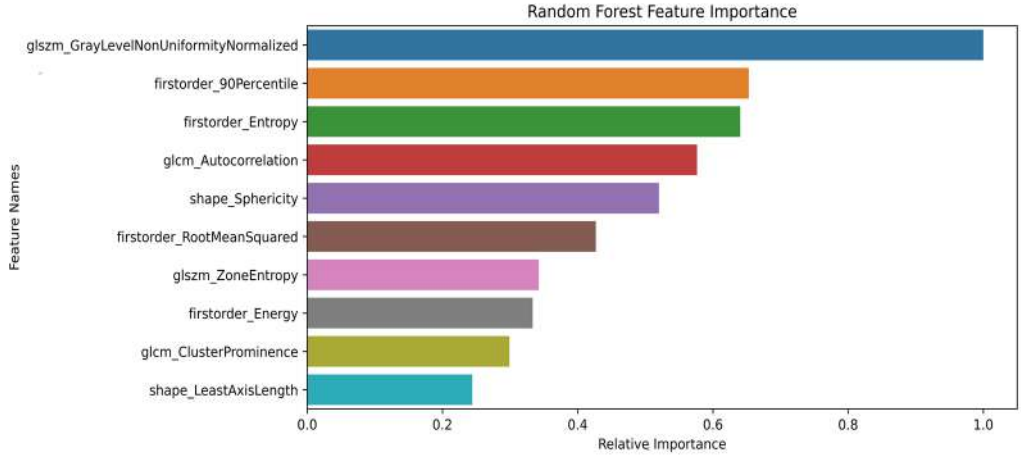

(a)

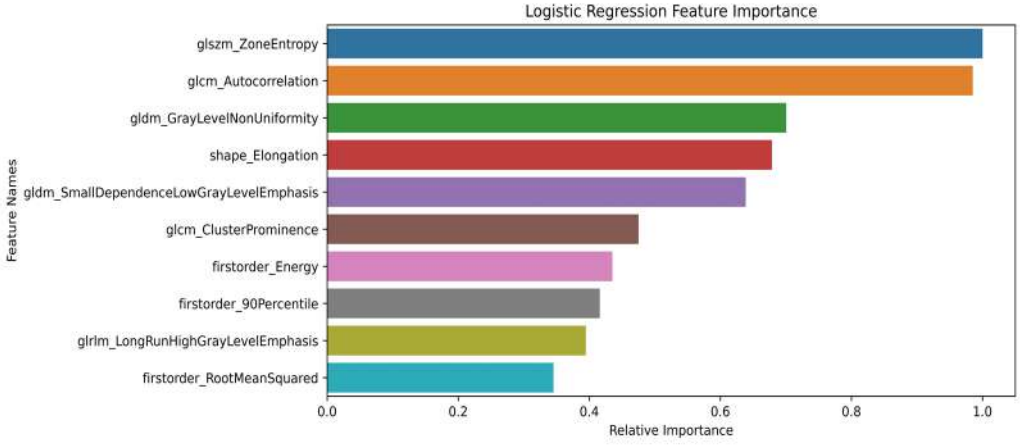

(b)

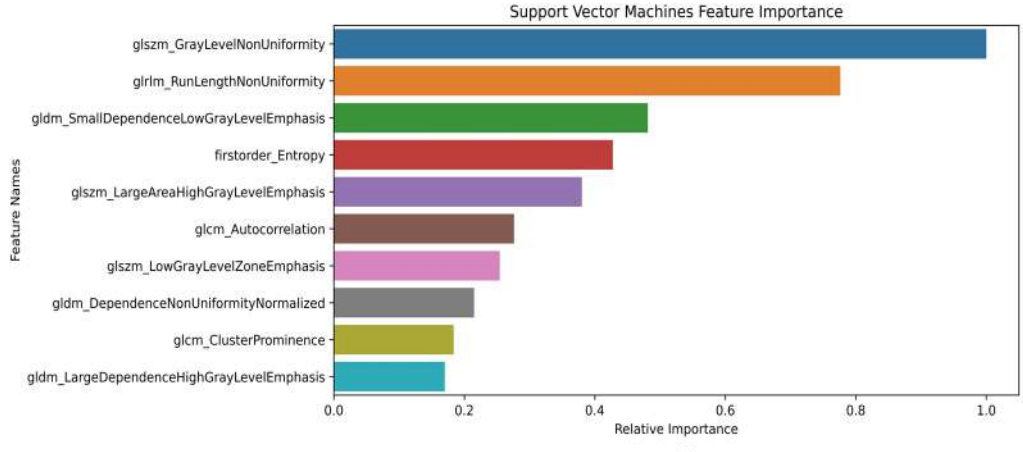

(c)

Figure 4. Feature importance of Random Forest (a), Logistic Regression (b), and Support Vector Machines (c) in COVID-19 mortality.

Table 4. Logistic Regression, Random Forest, and Support Vector Machines model's sensitivity, specificity, Accuracy, Precision, F1-score, and AUC for classification

Model	Sensitivity %95 CI	Specificity %95 CI	Accuracy %95 CI	Precision %95 CI	F1-Score %95 CI	AUC %95 CI
LR	0.88	0.62	0.74	0.55	0.67	0.80
	0.76-0.97	0.50-0.73	0.62-0.79	0.42-0.67	0.56-0.77	0.72-0.88
RF	0.75	0.82	0.78	0.68	0.71	0.85
	0.63-0.88	0.72-0.90	0.72-0.86	0.53-0.81	0.60-0.82	0.76-0.91
SVM	0.68	0.64	0.66	0.50	0.57	0.69
		0.54-0.75	0.57-0.74	0.38-0.63	0.44-0.68	0.59-0.79

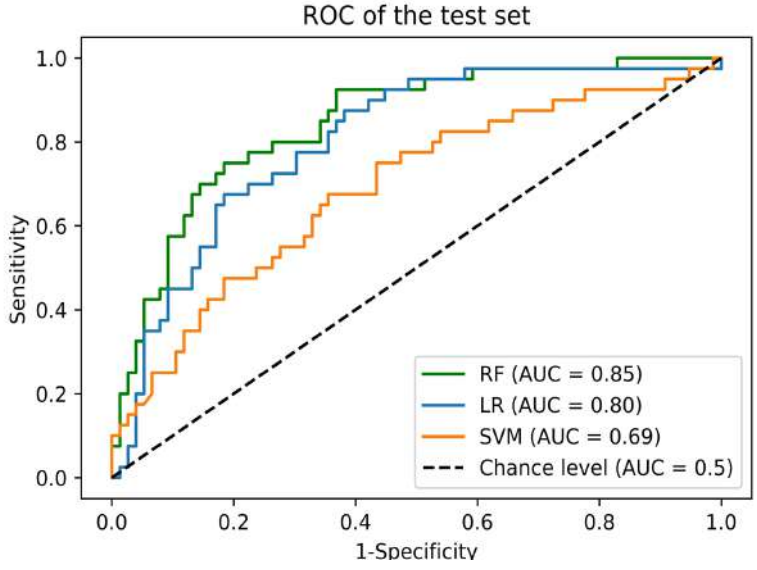

Figure 5. Area under the receiver operating characteristic curves (AUC) of Random Forest, Logistic Regression, and Support vector machines models.

precision, and F1-score were 0.80 (CI 95%: 0.72–0.88), 0.74, 0.88, 0.62, 0.55, and 0.67, respectively. The SVM model AUC, accuracy, sensitivity, specificity, precision, and F1-score were 0.69 (CI 95%: 0.59–0.79), 0.66, 0.68, 0.64, 0.5, and 0.57, respectively. In our work, precision and AUC report how well models predict patient deaths among patients classified as deceased and discriminate between deceased and recovered patients, respectively. Therefore, these are significant parameters for the models' evaluation.

Discussion

This study aimed to assess the predictive capability of our model in determining the mortality of COVID-19 patients using image processing techniques. We initially employed the class weighting technique within the training set to address the imbalanced classes in our dataset. We included a total of 577 patient images. We performed lung segmentation and accurately retrieved unique radiomics features. The dataset utilized for the suggested

approach was gathered from Imam Reza and Qaem hospitals and acquired with identical CT modalities. Due to collecting the dataset from different centers, we rescaled the voxel of images using isotropic algorithms. Due to imbalanced classes in our dataset, we used the class weight to automatically modify the importance of each group during the training process to ensure that the deceased group is given more attention.

Prognostic modeling is a crucial foundation for a deeper comprehension of the disease, handling it, observing, and determining the most effective therapeutic options. Several studies have demonstrated the efficacy of radiomics-based, clinical-based, or integrated models in predicting prognosis in COVID-19 patients.[20]

Qiu et al.[21] established a radiomics model designed to classify the intensity of COVID-19 infections. (indicating whether they are mild or severe) based on CT images. Their study encompassed 160 participants in the test cohort and demonstrated an AUC of 0.87. Their findings demonstrated the strong efficacy of the radiomics signature in assisting clinicians in improved patient management. An investigation conducted by Wang et al.[22] used several forms of information, including radiomics, clinical and integrated data, to utilize a comprehensive predictive model. The model accurately predicted patient assignments to either aggravation or improvement groups with an AUC of 0.84. Although their study showed encouraging outcomes, it lacked a substantial cohort.

Salimi et al.[23] examined algorithms' accuracy and diagnostic power, including random forests, in predicting mortality in patients with COVID-19. Their results showed that the random forest model best classifies observations based on the AUC. The random forest AUC and sensitivity were reported as 0.83 and 0.77, respectively. Therefore, their study results are similar to the current study's findings regarding the classification of observations using the random forest algorithm

Al-Areqi et al.[24] fitted the random forest model to the data in their study and calculated the precision, F1 score, and accuracy metrics. The findings of this study, similar to our own, demonstrated the impact of first order statistical characteristics on model fitting. In this study, the calculated amount based on the precision for the random forest model was reported as 0.96.

Kim[25] performed an analogous experiment using a radiomics model that utilized CT images. The model was then applied to 500 patients to classify them based on COVID-19 and Pneumonia. Their models demonstrated precise performance of the assigned task. (PPV=0.78 and AUC= 0.83).

Chao et al.[26] used several forms of information to develop a comprehensive predictive model, including radiomics-based features and clinical data. Their model achieved an AUC of 0.88, predicting whether patients would require surgery in the Intensive Care Unit (ICU). Tang[27] evaluated a random forest model of radiomics features and laboratory tests to classify patients into severe and non-severe groups. On their dataset of 118 patients, the model achieved a high level of performance (AUC = 0.98). Xu et al. [28] performed multicentric research to predict admission to the ICU, ventilation therapy, and mortality among COVID-19 patients. Radiomic features derived from CT scans were integrated with clinical and demographic data. The evaluation involved 1362 patients across

nine hospitals, demonstrating AUC values of 0.919, 0.916, and 0.853 for ventilation therapy, admission to the ICU, and mortality among patients, respectively. The radiomics model achieved an AUC of 0.80, 0.86, and 0.66 for the abovementioned outcomes. Also, they reached a precision of 0.24, 0.44, and 0.14, respectively. Many prior research studies were confronted with the shared constraint of a small sample size. To test our model's generalizability, we repeated our model's evaluation using stratified cross-validation. Predicting mortality requires the assessment of larger cohorts to create a generalizable model. Developing radiomics features can aid in prioritizing patients based on illness severity, given the considerable variability in COVID-19 symptoms across patients.

Our research has some limitations: Firstly, we excluded clinical data from model development. Secondly, we constructed a prognostic model using comprehensive lung radiomics features. Lastly, no explanation was provided for the biological interpretation of the radiomics features. The necessity to delve deeper into these findings in future research is well recognized.

Conclusion

We developed a radiomics model that provides a more accurate prediction of mortality in COVID-19 for estimating prognosis in COVID-19 patients. We provide evidence that radiomics features can serve as criteria for prognostic modeling in COVID-19. Modeling RF with radiomics features provided the highest performance compared to the LR and SVM models. Also, another principal finding of this research is that first order statistical features are worth more than other radiomics features.

Acknowledgments

The researchers express their gratitude and appreciation to the Statistics and Information Technology Management staff at Mashhad University of Medical Sciences for assisting researchers in data gathering. This paper is part of a thesis in the Department of Biostatistics in the School of Health of Mashhad University of Medical Sciences and was financially supported by the Vice-chancellor for Research and Technology, Mashhad University of Medical Sciences, Iran (project No. 4012129).

Conflicts of Interest

The authors declare no conflict of interest.

Reference

1. Omidi A, Shatizadeh Malekshahi S, Veisi P. Extrapulmonary Manifestations of Coronavirus Disease 2019: A Narrative Review. Journal of Arak University of Medical Sciences. 2020;23(5):604-13.

2. Nemati M, Ansary J, Nemati N. Machine-Learning Approaches in COVID-19 Survival Analysis and Discharge-Time Likelihood Prediction Using Clinical Data. Patterns (N Y). 2020;1(5):100074.

3. Organization WH. COVID-19 Weekly Epidemiological Update 2023 [Available from: https://www.who.int/publications/m/item/weekly-epidemiological-update-on-covid-19---25-january-2023.

4. Baik SM, Hong KS, Park DJ. Deep learning approach for early prediction of COVID-19 mortality using chest X-ray and electronic health records. BMC Bioinformatics. 2023;24(1):190.

5. Wang XV, Pinter JS, Liu Z, Wang L. A machine learning-based image processing approach for robotic assembly system. Procedia CIRP. 2021;104:906-11.

6. Tchito Tchapga C, Mih TA, Tchagna Kouanou A, Fozin Fonzin T, Kuetche Fogang P, Mezatio BA, et al. Biomedical Image Classification in a Big Data Architecture Using Machine Learning Algorithms. J Healthc Eng. 2021;2021:9998819.

7. Ronneberger O, Fischer P, Brox T. U-Net: Convolutional Networks for Biomedical Image Segmentation2015. 234-41 p.

8. Hatt M, Vallieres M, Visvikis D, Zwanenburg A. IBSI: an international community radiomics standardization initiative. Journal of Nuclear Medicine. 2018;59(supplement 1):287-.

9. Zhang Y-P, Zhang X-Y, Cheng Y-T, Li B, Teng X-Z, Zhang J, et al. Artificial intelligence-driven radiomics study in cancer: the role of feature engineering and modeling. Military Medical Research. 2023;10(1):22.

10. van Griethuysen JJM, Fedorov A, Parmar C, Hosny A, Aucoin N, Narayan V, et al. Computational Radiomics System to Decode the Radiographic Phenotype. Cancer Res. 2017;77(21):e104-e7.

11. Zwanenburg A, Vallières M, Abdalah MA, Aerts H, Andrearczyk V, Apte A, et al. The Image Biomarker Standardization Initiative: Standardized Quantitative Radiomics for High-Throughput Image-based Phenotyping. Radiology. 2020;295(2):328-38.

12. Saleh N, Ertunc HM, Saleh R, Rassam M. A Simple Mask Detection Model Based On A Multi-Layer Perception Neural Network2021. 1-5 p.

13. Zhang W, Guo Y, Jin Q. Radiomics and Its Feature Selection: A Review. Symmetry. 2023;15(10):1834.

14. Kraiem MS, Sánchez-Hernández F, Moreno-García MN. Selecting the Suitable Resampling Strategy for Imbalanced Data Classification Regarding Dataset Properties. An Approach Based on Association Models. Applied Sciences. 2021;11(18):8546.

15. Rymarczyk T, Kozłowski E, Kłosowski G, Niderla K. Logistic Regression for Machine Learning in Process Tomography. Sensors. 2019;19(15):3400.

16. Kumar D, Verma C, Singh PK, Raboaca MS, Felseghi R-A, Ghafoor KZ. Computational Statistics and Machine Learning Techniques for Effective Decision Making on Student's Employment for Real-Time. Mathematics. 2021;9(11):1166.

17. Janitza S, Hornung R. On the overestimation of random forest's out-of-bag error. PLoS One. 2018;13(8):e0201904.

18. Sansana J, Joswiak MN, Castillo I, Wang Z, Rendall R, Chiang LH, et al. Recent trends on hybrid modeling for Industry 4.0. Computers &

Chemical Engineering. 2021;151:107365.

19. Thanh Noi P, Kappas M. Comparison of Random Forest, k-Nearest Neighbor, and Support Vector Machine Classifiers for Land Cover Classification Using Sentinel-2 Imagery. Sensors (Basel). 2017;18(1).

20. Zhang K, Liu X, Shen J, Li Z, Sang Y, Wu X, et al. Clinically Applicable AI System for Accurate Diagnosis, Quantitative Measurements, and Prognosis of COVID-19 Pneumonia Using Computed Tomography. Cell. 2020;181(6):1423-33.e11.

21. Qiu J, Peng S, Yin J, Wang J, Jiang J, Li Z, et al. A Radiomics Signature to Quantitatively Analyze COVID-19-Infected Pulmonary Lesions. Interdiscip Sci. 2021;13(1):61-72.

22. Wang D, Huang C, Bao S, Fan T, Sun Z, Wang Y, et al. Study on the prognosis predictive model of COVID-19 patients based on CT radiomics. Sci Rep. 2021;11(1):11591.

23. Shiri I, Salimi Y, Pakbin M, Hajianfar G, Avval AH, Sanaat A, et al. COVID-19 prognostic modeling using CT radiomic features and machine learning algorithms: Analysis of a multi-institutional dataset of 14,339 patients. Comput Biol Med. 2022;145:105467.

24. Al-Areqi F, Konyar MZ. Effectiveness evaluation of different feature extraction methods for classification of covid-19 from computed tomography images: A high accuracy classification study. Biomedical Signal Processing and Control. 2022;76:103662.

25. Kim YJ. Machine Learning Model Based on Radiomic Features for Differentiation between COVID-19 and Pneumonia on Chest X-ray. Sensors (Basel). 2022;22(17).

26. Chao H, Fang X, Zhang J, Homayounieh F, Arru CD, Digumarthy SR, et al. Integrative analysis for COVID-19 patient outcome prediction. Med Image Anal. 2021;67:101844.

27. Tang Z, Zhao W, Xie X, Zhong Z, Shi F, Ma T, et al. Severity assessment of COVID-19 using CT image features and laboratory indices. Phys Med Biol. 2021;66(3):035015.

28. Xu Q, Zhan X, Zhou Z, Li Y, Xie P, Zhang S, et al. CT-based Rapid Triage of COVID-19 Patients: Risk Prediction and Progression Estimation of ICU Admission, Mechanical Ventilation, and Death of Hospitalized Patients. medRxiv. 2020.